Identification of two clinical hepatocellular carcinoma patient phenotypes

[1*]Brian I. Carr MD, FRCP, PhD and [2*]Petr Pancoska PhD

[1]Department of Liver Tumor Biology IRCCS de Bellis, National Institute for Digestive Diseases, Castellana Grotte , BA, Italy; [2]Center for Craniofacial and Dental Genetics, University of Pittsburgh, Pittsburgh, PA, USA.

Running title: Two HCC phenotypes

Key Words: HCC, tumor mass, portal vein thrombosis, AFP

Author contributions: Carr: idea, writing; Pancoska, statistical analysis.

Abbreviations: HCC, hepatocellular carcinoma; AFP, alpha-fetoprotein; PVT, portal vein thrombosis, Hgb, hemoglobin, plts, platelets, WBC, white blood count; INR, international normalized ratio; CAT, computerized axial tomogram; HBV, hepatitis B virus; HCV, hepatitis C virus; L, large; S, small.

Disclosures: none.

*Both authors contributed equally

Grant support: ERZ-CZ LL1201 (CORES) to PP.

Correspondence: Brian I. Carr MD, FRCP, PhD

IRCCS 'S. de Bellis', via Turi 27, 70013 Castellana Grotte (BA), Italy

Tel. 39 080 4994603; Fax. 39 080 4994313

E-mail: brianicarr@hotmail.com

Abstract

Background. Standard liver function parameter levels and tumor indices were analyzed using Network Phenotyping Strategy (NPS), a graph-theory based approach, which compares personal patterns of complete relationships between clinical data to reference patterns with significant association to disease outcome. We previously applied NPS to Taiwan hepatocellular cancer (HCC) patients and recognized two clinical phenotypes, S and L, differing in the size and tumor nodule numbers.

Aims. To validate the applicability of the NPS-based HCC S/L classification on an independent European HCC cohort, for which survival information was additionally available.

Results. Patients with S and L phenotypes, recognized by the same data processing as previously, had 1.5x larger mean tumor masses in L relative to S, $p=6x10^{-16}$. S-phenotype patients had typically 1.7x longer survival compared to L-phenotype. NPS integrated liver- and tumor factors. Cirrhosis associated thrombocytopenia was typical for smaller S-tumors. Hepatic inflammation and tumor factors contributed to more aggressive L tumors, with parenchymal destruction and shorter survival.

Summary. NPS provides integrative interpretation for HCC behavior, identifying by clinical parameter patterns two tumor and survival phenotypes. The NPS classifier was implemented as an application for web browsers and is available upon request

Introduction

Previous work has shown that 2 general processes contribute to HCC prognosis. They are liver damage indices, such as bilirubin, prothrombin time and AST , as well as tumor biology indices, such as tumor size, tumor number, presence of PVT and blood AFP levels (1-5). These 2 general processes may affect one another (6-8). Non disease factors such as gender and age can also influence HCC outcomes (9-10), suggesting that any individual disease parameter needs to be considered within a total clinical context. Prognostically significant factors may actually function in part through interaction with multiple other tumor and host parameters, as the basis for this context. This context might even provide patient personalization to individually measured parameters. Thus, a given level of bilirubin or tumor diameter might have a different significance in different total clinical contexts.

We thus considered standard liver function parameter levels and commonly assessed tumor indices, within the total context of the relationships between all of the parameters together of individual patients. The net result, obtained using a large cohort of Chinese HCC patients in Taiwan (n=4139) in a training set was that unmanageably complex individual patient parameter relationships were captured in just 9 relationship patterns, and were significantly related to disease outcome (11). Within these 9 relationship patterns, there were 2 distinct general sub-sets of parameter level and relationship patterns, closeness or large distance from them being associated with significantly different tumor masses. We called these two phenotype subgroups of HCC patients with different clinical characteristics 'S' and 'L', for 'small' and 'large' tumor mass. However, survival data was not available for that analysis. In the current paper, we have used an Italian database of 1619 HCC patients with known survival outcomes, to validate that these 2 characteristic pattern sets and the personalized characterization of the closeness and differences from these clinical patterns, can also provide significantly different tumor mass outcomes and that patients with these two different phenotype and clinical relationship patterns have significantly different survival outcomes.

Methods

Data collection. We retrospectively analyzed prospectively-collected data in the Italian Liver Cancer (ITA.LI.CA) study group database of HCC patients accrued at 11 centers (12). 2773 newly diagnosed HCC patients had full baseline parameter data, including radiology of maximum tumor diameter

(MTD), number of tumor nodules and presence of PVT; demographics (gender, age, alcohol history, presence of hepatitis B or C); blood counts (hemoglobin, white cells, platelets, prothrombin time); blood AFP and routine liver function tests, (total bilirubin, AST, ALKP, GGTP, albumin). ITA.LI.CA database management conforms to Italian legislation on privacy and this study conforms to the ethical guidelines of the Declaration of Helsinki. Approval for the study on de-identified patients was obtained by the Institutional Review Board of participating centers.

Data processing. The clinical parameter data were processed exactly as previously (11,13). The data processing summary and parameter-relationship pattern based classification model is shown in Fig 1. In the training set data from Taiwan (Fig. 1a), the screening "raw" clinical data was converted into 4139 individual patient profiles (Fig. 1b). In designing these profiles we first used graph-theory algorithm to identify pairs of collectively most correlated liver function and tumor growth-related parameters (platelets/AFP, AST/ALT and bilirubin/INR), each pair being used as one component of the individual clinical profiles. This step incorporated explicitly the strongest inter-relationships (pairwise correlations) within the data and thus reduced the number of parameter-parameter relationships to be considered. The paired parameter values were dichotomized into high (H) and low (L) using terciles (L corresponded to 2/3 of patient's cohort with the lowest paired parameter values, H to the upper 1/3). This approach allowed direct combination with the rest of the clinical data (demographic, hepatitis, portal vein thrombosis) in a unified quantitative scheme. All individual clinical profiles were collected into 10-partite network $\boldsymbol{K_{10}}$ (Fig.1c) with edges weighted by the co-occurrence frequencies quantifying all relationships between all parameters. This study network was then used to generate reference relationship patterns, relative to which we compared the actual individual clinical profiles, using specific algorithm (11,13). It was found (Fig.1d) that the training set network was a weighted combination of 19 reference relationship patterns. By definition, these 19 reference relationship patterns collect independently all pairwise context relationships (such as when males have PVT present, when the PVT is present with AFP and platelet levels in the high, upper tercile subgroup etc., covering the complete set of all 45 pairwise relationships between the 10 parameter groups (Fig.1a). We collected into the respective reference relationship patterns those pairwise parameter relationship patterns, which were observed in the study data with identical frequencies. This guarantees that results are independent of the parameter ordering in the clinical profile. In the final step of the clinical data transformation, we compared actual individual clinical profiles for each patient with these reference relationship patterns and characterized the closeness

between them by counting differences (see Fig.1e). In this way, we arrived at our new characterization of the context relationships in the study data, quantified by the set of 19 "distances" from respective ideal reference clinical relationship patterns. We previously found, using the variable selection in combination with the logistic regression least squares optimization, that distances from only 9 out of these 19 reference relationship patterns are significantly associated with tumor mass (Fig. 1d) as the HCC outcome parameter.

For the purpose of this validation study, we converted the data from this cohort of 1619 HCC patients into their individual clinical profiles identically to the training set data processing. We then computed the distances of every individual clinical profile from 9 significant reference relationship patterns (Fig.1e shows an example of this computation for one concrete patient). For each patient, the individual 9 distances from the common reference relationship patterns were used as independent variables in the logistic regression equation resulted from the training set data processing. Based on the odds comparisons, each patient was classified as L- or S- phenotype. This resulted in 772 patients (48%) in the L group and 847 patients (52%) in the S group.

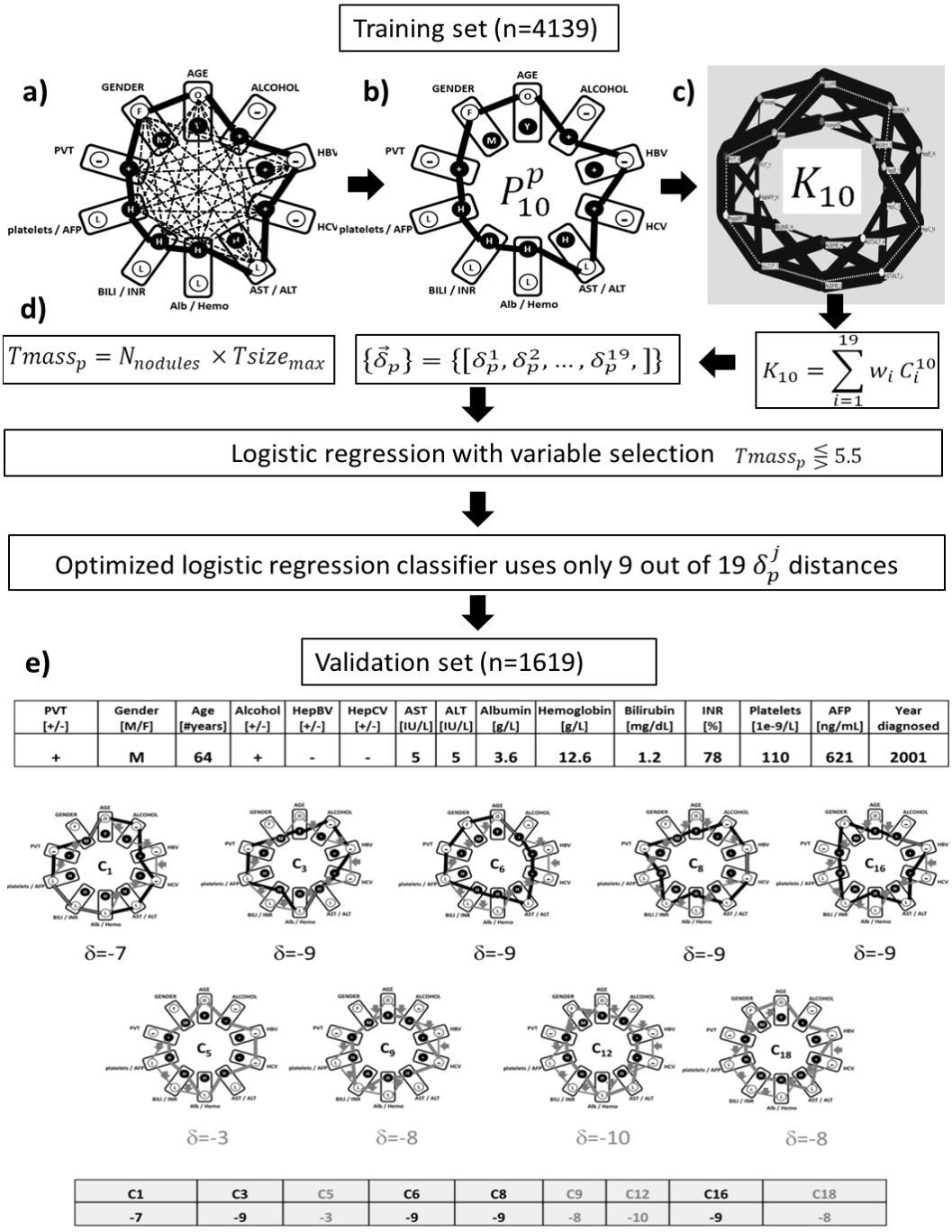

Figure 1. Scheme of the Network Phenotyping Strategy processing of HCC data. **a)** Scheme of all relationships between the clinical data levels and statuses, compiled into 10-partite graph (see Methods for details). **b)** Equivalent representation of the complete information about all data relationship for a concrete patient ***p*** in simpler 10-partite clinical profile. **c)** Union of clinical profiles for all patients results in 10-partite study network. Edge thicknesses are proportional to the occurrence frequency of every binary relationship in the training (Taiwan) study. **d)** Flow chart of the analysis steps (see Methods and ref. [Taiwan]) **e)** Example of conversion of actual clinical data for one patient from this validation study (top table) into vector of distances from the nine reference relationship pattern, found as significant for S and L tumor phenotype classification in ref [Taiwan]. The vector of these 9 pattern-pattern distances is converted by logistic regression into diagnosis of S or L tumor phenotype for each patient.

To characterize the clinical differences between the S and L subgroups, we used statistical testing of means of outcome parameter distributions (SigmaPlot 11), Kaplan-Meier survival analysis (survival package in R, version 2.15.1) and moving average processing with windows of 61 patients (implemented in Maple 12).

Results

Independent validation of S and L clinical phenotyping

Fig. 2a presents the box plots of the distributions of the tumor masses for patients from the

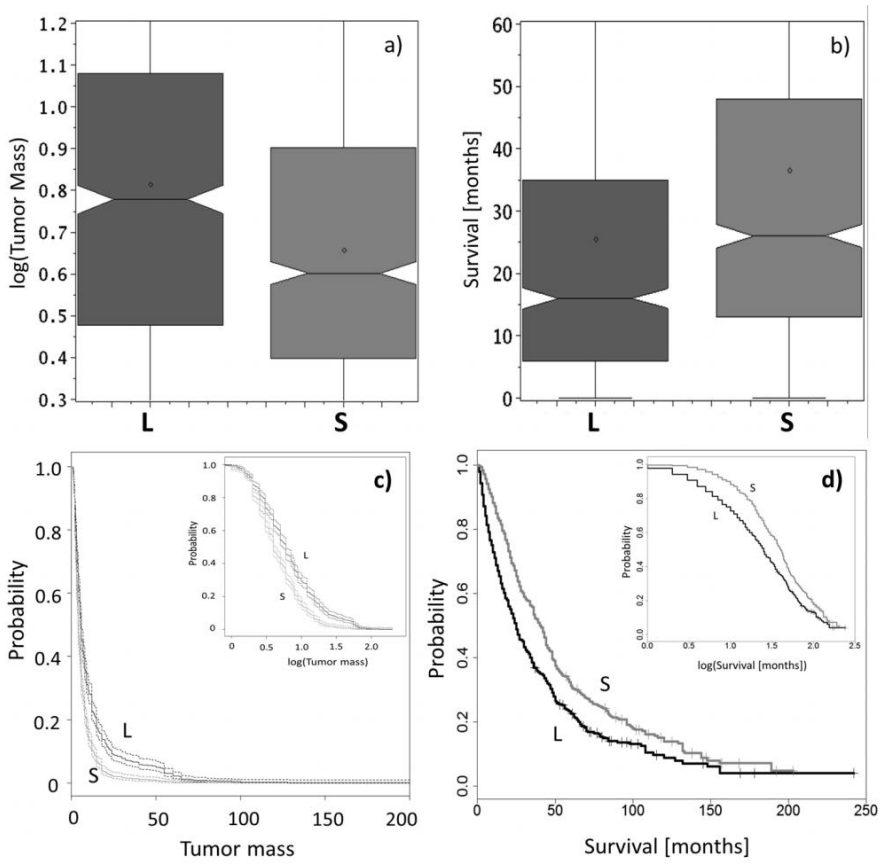

Figure 2. Validation of HCC outcome differences for patients with S and L tumor phenotypes. Boxplots of the differences in the **a)** tumor masses and **b)** in the overall survival for patients with the S and L phenotypes. Kaplan-Meier plots of the significant differences between the probabilities to find equivalent **c)** tumor masses and **d)** overall survivals for patients with the S and L phenotypes.

test set in the S and L phenotypes. The means of these distributions were significantly different, $p=6 \times 10^{-16}$. The significance of this outcome of the 2 HCC groups independently validates the significant

tumor mass differences between these two HCC tumor phenotypes, identified by our relationship pattern analysis in the Chinese patient training dataset.

Although the difference of means was highly statistically significant, there was still significant overlap in the distribution of the tumor masses in the 2 groups. The overlap reflects the complexity of the HCC phenotype together with the unknown point on the course of the HCC development at the point of any individual patient diagnosis. By inspecting these distributions separately in S and L phenotype subgroups we found that probability of finding the same tumor mass in the 2 HCC groups was significantly different (Fig. 2c, differences between the probabilities are larger than 2 times 95% confidence interval of the respective probability estimates). We therefore conclude that, for a given tumor mass, patients from the S group are significantly more likely to be in a more advanced phase of HCC progression than in the L group.

Survival was also analyzed in two ways. First, we tested the statistical significance of the differences in means of the survival distributions, computed separately for the two groups of S and L phenotype patients (see box plots, Fig. 2b). The mean for S patients was 24 months, for L the mean survival was 14 months (difference significant, $p = 10^{-21}$). Thus S-phenotype patient had 1.7 times longer mean survival compared to L-phenotype. Second, we performed the Kaplan-Meier survival analysis and found significantly different probabilities of survival in the S and L HCC phenotype patient subgroups (see Fig. 2d). The typical separation of the S- and L- survival provability curves is statistically significant, exceeding double of the 95% confidence interval of the two estimated survival probabilities.

Tumor mass relationships in S and L groups. The identification of S and L subgroups, differing in the survival, resulted from the analysis of relationship patterns between clinical liver function and

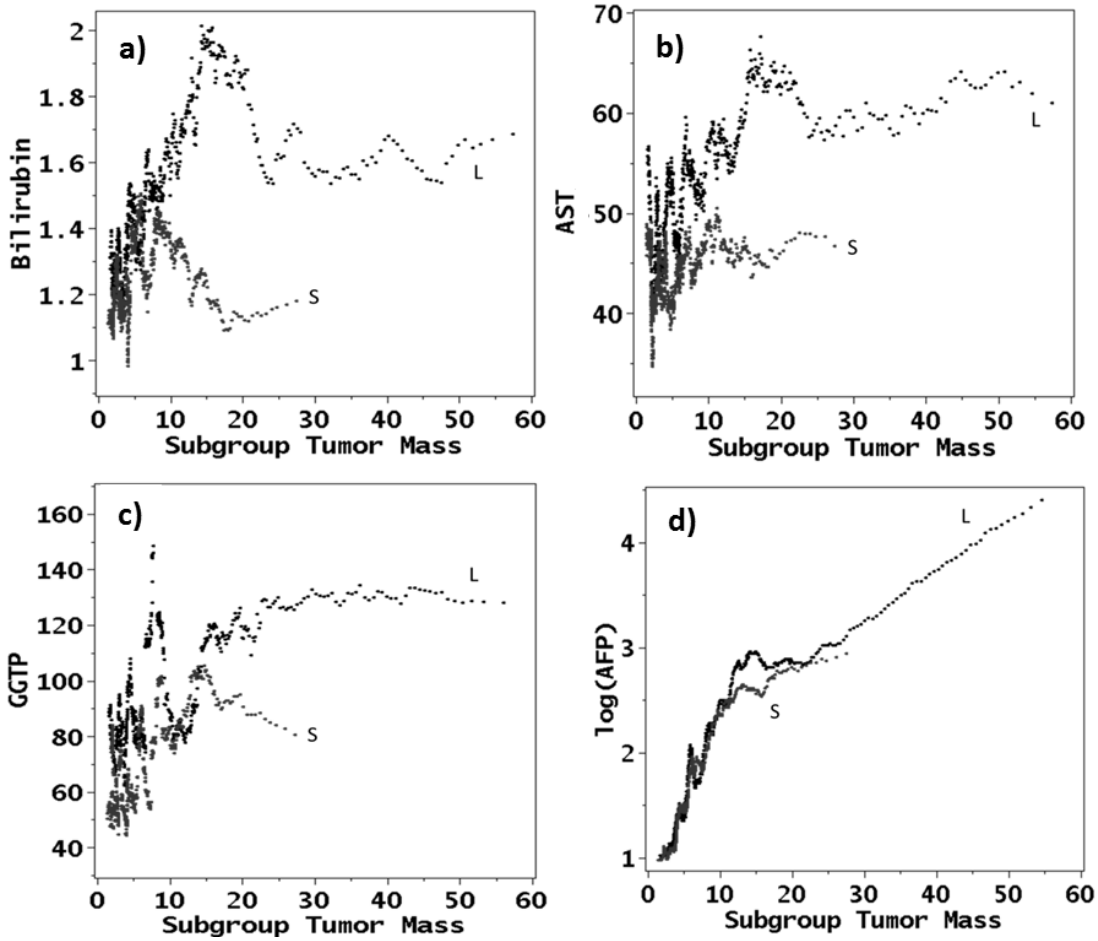

Figure 3. Trends between typical values of tumor masses and various clinical parameters as they differ for S and L phenotypes.

tumor parameters. This provides the basis for analysis of the functional differences between the 2 phenotypes, because we can now analyze separately the patients from the two well defined and characterized phenotypic groups, S and L. To visualize the dominant trends in relationships between the screening and outcome clinical variables, moving average processing of biologically interesting parameter pairs was used. In the first part of this analysis step, relationship between screening clinical parameters and tumor mass were inspected. Patients were first ordered according to tumor mass, separately in S and L phenotype groups and then the screening clinical parameter and tumor mass values were processed by the moving average to reveal dominant trend between the data in the pair. The relationships between tumor mass and both internal tumor factors (AFP) and liver factors

(bilirubin, AST, GGTP) were studied. Fig 3a shows that the typical trends between bilirubin and tumor mass are different between S and L phenotypes. Overall, there were higher typical bilirubin levels in S subgroup than in L, for a given tumor mass. For both groups, bilirubin increased with increasing mass for small tumors. However, with increasing tumor mass, there appeared to be no further relationship between increasing mass and bilirubin levels, accompanied by a lowering of typical bilirubin levels. This transition in the relationship between mass and bilirubin occurred at smaller tumor masses in S compared with L. This lack of further increase in typical bilirubin levels as the tumors continued to grow, suggested to us, that factors internal to the tumor were dominant in the increasing tumor growth. This looks like a plausible functional hypothesis, but evidence from just one (bilirubin) clinical variable is insufficient. The novelty of our characterization of S and L HCC tumor phenotypes is in recognizing them from the differences in the clinical data relationship patterns in the two groups, instead from the conventional normal/elevated clinical variable level approach. Thus, any functional interpretation of what is observed for single clinical variable in relationship to the tumor characteristic or disease outcome has to be contrasted and confirmed by examining the trends in other liver parameters. Following these novel ideas, we therefore examined trends revealed by the moving-average processing for AST and GGTP with respect to increasing tumor mass. They showed remarkable similarities to the trends for bilirubin (Figs 3b and 3c).

These results also showed that beyond a certain small tumor mass, continued tumor growth was not accompanied by increased evidence for tumor damage. In this multi-variable context, it is interesting that the examination of AFP trends showed increased levels with increasing tumor mass and was comparable for both S and L groups. AFP thus appears to monitor tumor growth through its full range, unlike the changes in liver function parameters. Another observation was that beyond a certain point of tumor growth, further increase in tumor mass was associated with a lesser increase in AFP per unit increase in tumor mass. This change in the slope of the tumor mass - AFP trend occurred at the same tumor mass as the decrease in related trend for both bilirubin and AST. All these results combined and interpreted in mutual context, are consistent with the hypothesis that with further tumor growth, the contribution from liver factors decreased and the internal tumor factors regulating growth remained increasing, reflected in the lesser response of AFP to further increase in tumor mass. An analysis was done for trends of liver parameters for increasing AFP instead of increasing tumor mass. The results were very similar (data not shown).

AFP relationships

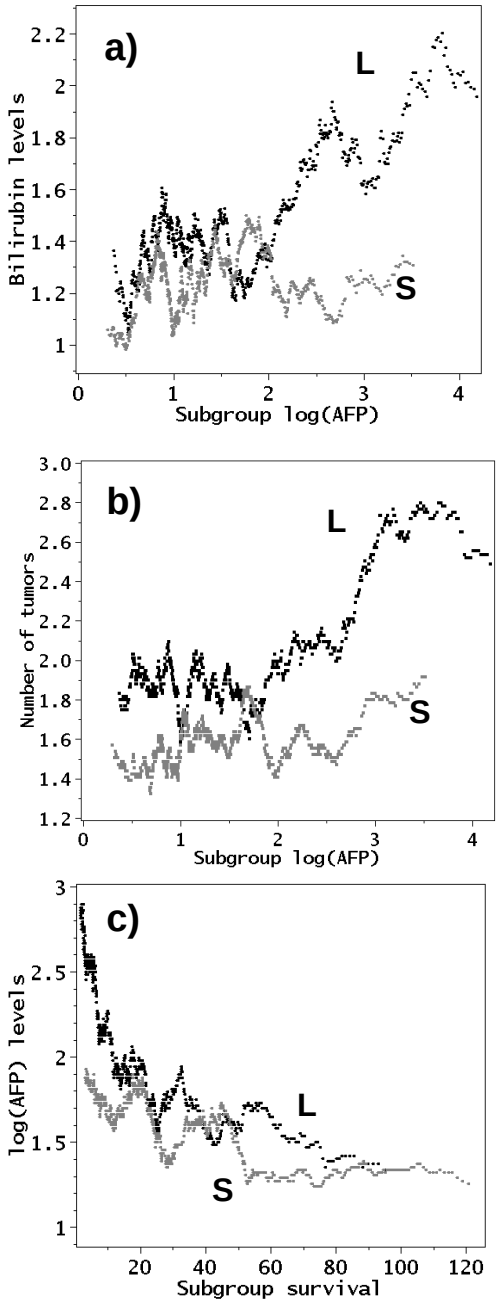

Figure 4. Trends between typical values of AFP levels in log-scale and **a)** bilirubin, **b)** tumor numbers and **c)** survival as they differ for S and L phenotypes.

Given the finding of AFP as a monitor of HCC growth, above, we next analyzed the typical levels of liver function parameters for patients with comparable AFP levels, separately for S and L phenotype groups. We analyzed patterns in bilirubin, tumor numbers and survival with respect to AFP levels (Fig. 4). We found that tumor tumors increased with increasing AFP levels in both phenotypes. However, there was typically a smaller number of tumors in S compared with L phenotype, for patients with comparable AFP levels (Fig. 4A). Furthermore, beyond AFP log 2.5 levels, tumor numbers increased at a greater rate in L patients than in S. Thus, the increase in tumor mass from AFP log 0 to 2.5 in Fig 3 above, is likely due to increase in tumor size alone, but above this AFP level, the increase in tumor mass also has a contribution from increased number of tumor nodules, mainly in L. The increase in numbers of tumors in S was only modest. Increasing AFP levels were associated with decreasing survival. Thus, for a given similarity of survival, L patients had higher AFP than S patients (Fig. 4B). Given the importance of both liver and tumor factors in HCC, we next plotted the trends in bilirubin levels as a function of increasing AFP levels. We found incoherency between bilirubin and AFP typical levels up to log AFP 2.0. Thereafter, this trend continued for S patients, but not L, in whom increasing AFP was followed by increasing bilirubin levels (Fig. 4D). In Fig 3A, increase in tumor mass was not associated with increase in bilirubin levels

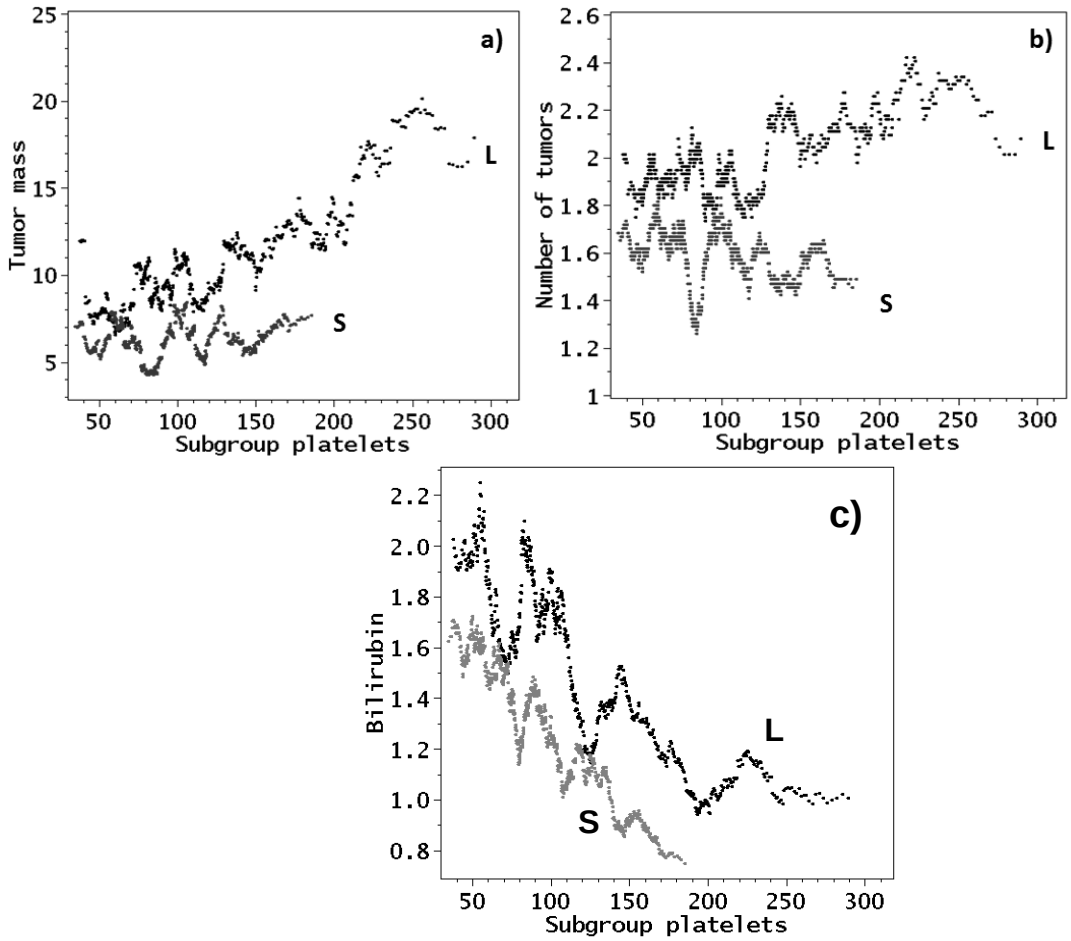

Figure 5. Trends between typical values of platelet levels and **a)** tumor mass, **b)** tumor numbers and **c)** bilirubin as they differ for S and L phenotypes.

in S patients. This transition in AFP levels around log 2 corresponds to the change in the rate of increase per unit of tumor mass and also to the point at which bilirubin/tumor mass level changes diverged between S and L in Fig. 3.

Platelet relationships.

After our initial analysis of complete correlations between all parameters (Methods), platelets and AFP were part of the set of 4 pairs with highest correlations. Examination of patterns of trends between platelets and other parameter were examined (Fig. 5). We found no correlation of platelets with tumor mass or number for S patients. However, for L patients there was a linear trend between typical platelet values and tumor mass or number of nodules in L patients. We found a U-shaped pattern in the trends for platelets with increasing AFP, with a turning point at log AFP 1.5 to 2. In addition, platelet levels were systematically lower in S than L. This transition point also corresponds to transitions in other parameters. In the majority of the AFP range, from log 1.5 to log 3 levels, there was an increase in platelets with increase in AFP. At the highest AFP levels at >log 2.5, where bilirubin levels also are increasing (Fig. 4), the platelets start to decrease, consistent with the bilirubin/platelet relationship of liver failure.

Discussion

We have previously used a network phenotyping strategy (NPS) on a large cohort of Chinese HCC patients, to show that analysis of parameter relationship patterns could identify 2 sets of HCC patient phenotypes, called S and L. The results showed that if the parameter values were considered in the context of all other parameters, that for a given tumor mass, we could identify 2 possible sets of clinical phenotypic patterns. Survival data was not available for that analysis. We have now extended that initial study, by examining whether this approach could be used to examine a large and completely different HCC cohort amongst another ethnic patient HCC group, using the identical method of data processing and the quantitative model. We again found that the total cohort could be cleanly separated into S and L phenotypes, each associated with significantly different tumor masses and survival.

Main findings of this paper include the relationships between various parameter patterns and total tumor mass (Fig. 2). Three parameter trends in relation to tumor mass showed distinct differences between S and L: Trends for bilirubin, AST and GGTP showed an increase with increasing tumor mass for L, but not for S patients, beyond limited tumor mass, However, the trends for AFP were different, since there was a general non-linear increase in AFP with tumor mass for both S and L patients. We interpret this to signify the direct importance of AFP in growth of both S and L tumors. By contrast, we suppose that involvement of bilirubin, AST and GGTP with tumor mass is more indirect. Thus, AFP could be a mediator of internally-derived growth of HCCs (oncogenes, growth factors), whether of S or L phenotype. By contrast, the other 3 liver parameters might reflect the tumor micro-environment that permits or modulates HCC growth and behavior. We found that trends for bilirubin, AST and GGTP were all higher for the larger and more aggressive HCC L phenotype, that were associated with shorter survival than S phenotype patients. This NPS approach thus synthesizes and integrates both liver and tumor factors.

The analysis reveals both pattern and complexity in HCC phenotypes. Both liver and tumor factors are well-described in HCC prognosis. Our relationship pattern based processing of the data permitted us to discern 2 distinct clinical HCC phenotypes. Inspecting typical trends between different parameters, we found increasing trends in L phenotypes for several parameters, but constancy in parameter trends for S phenotype, which suggests some possible mechanistic interpretations. Most HCCs arise on the basis of hepatic inflammation with some degree of associated cirrhosis (14, 15, 16), and is consistent with elevated bilirubin, AST and GGTP for the S and L tumors. The portal hypertension and splenomegaly

associated thrombocytopenia appeared mainly as a feature of S tumors, reflecting small HCC development in cirrhosis. As S tumors grew, they did not appear to further worsen the liver function parameters, possibly due to their significantly smaller size compared to L tumors. The parameter trends were more complex in L tumors, likely due to multiple factors, including hepatic inflammation and endogenous tumor factors. Unlike S, the L phenotype patients predominantly did not have thrombocytopenia. We hypothesize than in L, unlike S patients, the known platelet-derived tumor growth factors (17-24) and inflammation-associated cytokines (25,26) may play a role in the expansion of the growing tumor mass. There is an inverse relationship between bilirubin and platelet levels in portal hypertension, and our patients were no exception (Fig. 5C). However, there are also other causes of elevated bilirubin levels, which must be involved to explain the increasing bilirubin levels associated with large tumors seen in Fig. 3A. These include both inflammation (Figs 3A,B, and C) as well as parenchymal liver destruction by larger tumor masses. S and L differ in the relative contributions of these mechanisms, recognizable by their different patterns.

Figure Legends

Figure 1. Scheme of the Network Phenotyping Strategy processing of HCC data. a) Scheme of all relationships between the clinical data levels and statuses, compiled into 10-partite graph (see Methods for details). **b)** Equivalent representation of the complete information about all data relationship for a concrete patient ***p*** in simpler 10-partite clinical profile. **c)** Union of clinical profiles for all patients results in 10-partite study network. Edge thicknesses are proportional to the occurrence frequency of every binary relationship in the training (Taiwan) study. **d)** Flow chart of the analysis steps (see Methods and ref. [Taiwan]) **e)** Example of conversion of actual clinical data for one patient from this validation study (top table) into vector of distances from the nine reference relationship pattern, found as significant for S and L tumor phenotype classification in ref [Taiwan]. The vector of these 9 pattern-pattern distances is converted by logistic regression into diagnosis of S or L tumor phenotype for each patient (see Excel implementation of this NPS-based HCC subtype classification, provided as supplementary file to this paper).

Figure 2. Validation of HCC outcome differences for patients with S and L tumor phenotypes. Boxplots of the differences in the a) tumor masses and b) in the overall survival for patients with the S and L phenotypes. Kaplan-Meier plots of the significant differences between the probabilities to find equivalent **c)** tumor masses and **d)** overall survivals for patients with the S and L phenotypes.

Figure 3. Trends between typical values of tumor masses and various clinical parameters as they differ for S and L phenotypes.

Figure 4. Trends between typical values of AFP levels in log-scale and **a)** bilirubin, **b)** tumor numbers and **c)** survival as they differ for S and L phenotypes.

Figure 5. Trends between typical values of platelet levels and **a)** tumor mass, **b)** tumor numbers and **c)** bilirubin as they differ for S and L phenotypes.

Appendix

Phenotypic Classifier: Implementation of patient classification into S and L HCC phenotypes

References

1. Qin LX**,**Tang ZY**.** The prognostic significance of clinical and pathological features in hepatocellular carcinoma. World J Gastroenterol. 2002 Apr;8(2):193-9.
2. Cabibbo G, Maida M, Genco C et. Al. Natural history of untreatable hepatocellular carcinoma: A retrospective cohort study. World J Hepatol. 2012;4:256-61
3. Lee YH, Hsu CY, Hsia CY et. al. A prognostic model for patients with hepatocellular carcinoma within the Milan criteria undergoing non-transplant therapies, based on 1106 patients. Aliment Pharmacol Ther. 2012;36:551-9
4. Park KW, Park JW, Choi JI et. al. Survival analysis of 904 patients with hepatocellular carcinoma in a hepatitis B virus-endemic area. J Gastroenterol Hepatol. 2008;23:467-73.
5. Cabibbo G, Genco C, Di Marco V et. al. Predicting survival in patients with hepatocellular carcinoma treated by transarterial chemoembolisation. Aliment Pharmacol Ther. 2011;34:196-204
6. Hoshida, Y., Villanueva, A., Kobayashi, M., Peix, J., Chiang, D.Y., Camargo, A., Gupta, S., Moore, J., Wrobel, M.J., Lerner, J. *et al.* (2008) Gene expression in fixed tissues and outcome in hepatocellular carcinoma. *The New England journal of medicine*, 359, 1995-2004.
7. Leonardi, G.C., Candido, S., Cervello, M., Nicolosi, D., Raiti, F., Travali, S., Spandidos, D.A. and Libra, M. (2012) The tumor microenvironment in hepatocellular carcinoma (review). *International journal of oncology*, 40, 1733-1747.
8. Utsunomiya, T., Shimada, M., Imura, S., Morine, Y., Ikemoto, T. and Mori, M. (2010) Molecular signatures of noncancerous liver tissue can predict the risk for late recurrence of hepatocellular carcinoma. *Journal of gastroenterology*, 45, 146-152.
9. Gender-based outcomes differences in unresectable hepatocellular carcinoma. Buch SC, Kondragunta V, Branch RA, Carr BI. Hepatol Int. 2008;2:95-101

10. Carr, B.I., Pancoska, P. and Branch, R.A. HCC in older patients. *Digestive diseases and sciences* 2010; 55, 3584-3590.

11.Phenotypic categorization and profiles of Small and Large hepatocellular carcinomas. Pancoska P, Lu S-N, Carr BI. Journal of Gastrointestinal & Digestive System 2013, S12: 001,doi:10.4172/2161-069X.S12-001

12. Santi V, Buccione D, Di Micoli A et. Al. The changing scenario of hepatocellular carcinoma over the last two decades in Italy. J. Hepatol. 2012; 56: 397-405

13. Pancoska, P., Carr, B.I. and Branch, R.A. (2010) Network-based analysis of survival for unresectable hepatocellular carcinoma. *Seminars in oncology*, 37, 170-181.

14. Della Corte C, Aghemo A, Colombo M. Individualized hepatocellular carcinoma risk: the challenges for designing successful chemoprevention strategies. World J Gastroenterol. 2013;19:1359-71

15. Karagozian R, Baker E, Houranieh A, Leavitt D, Baffy G. Risk Profile of Hepatocellular Carcinoma Reveals Dichotomy among US Veterans. J Gastrointest Cancer. 2013 Apr 23. Epub

16. Mittal S, El-Serag HB. Epidemiology of Hepatocellular Carcinoma: Consider the Population. J Clin Gastroenterol. 2013 Apr 29. Epub

17. Yang ZF, Ho DW, Lau CK et. al. Platelet activation during tumor development, the potential role of BDNF-TrkB autocrine loop. Biochem Biophys Res Commun. 2006;346:981-5

18. Zhou J, Tang YZ, Fan J et al. Expression of platelet-derived endothelial cell growth factor and vascular endothelial growth factor in hepatocellular carcinoma and portal vein tumor thrombus. J. Cancer Res. Clin. Oncol. 2000; 126: 57-61

19. Stock P, Monga D, Tan X et al. Platelet-derived growth factor receptor-alpha: a novel therapeutic target in human hepatocellular cancer. Mol. Cancer Ther. 2007:6: 1932-41

20. Campbell JS, Hughes SD, Gilbertson DG et al. Platelet-derived growth factor C induces liver fibrosis, steatosis and hepatocellular carcinoma. Proc. Natl. Acad. Sci. USA 2005; 102: 3389-94

21. Soll C, Jang JH, Riener MD et al. Serotonin promotes tumor growth in human hepatocellular cancer. Hepatology 2010; 51:1244-54

22. Gauglhofer C, Sagmeister S, Schrottmaier W et al Up-regulation of the fibroblast growth factor 8 subfamily in human hepatocellular carcinoma for cell survival and neoangiogenesis. Hepatology. 2011;53:854-64.

23. Miura S, Mitsuhashi N, Shimizu H et al Fibroblast growth factor 19 expression correlates with tumor progression and poorer prognosis of hepatocellular carcinoma. BMC Cancer. 2012 ;12:56.

24. French DM, Lin BC, Wang M et al. Targeting FGFR4 inhibits hepatocellular carcinoma in preclinical mouse models. PLoS One. 2012;7:e36713.

25. Sitia G, Aiolfi R, Di Lucia P et al. Antiplatelet therapy prevents hepatocellular carcinoma and improves survival in a mouse model of chronic hepatitis B. Proc Natl Acad Sci U S A. 2012;109:E2165-72

26. Spengler U.Hepatic microcirculation: a critical but neglected factor for the outcome of viral hepatitis. J Hepatol. 2009;50:631-3